Cell, Vol. 110, 789–799, September 20, 2002, Copyright ©2002 by Cell Press

Adenovirus Fiber Disrupts CAR-Mediated Intercellular Adhesion Allowing Virus Escape

Robert W. Walters,[1,2,3] Paul Freimuth,[4] Thomas O. Moninger,[1,2] Ingrid Ganske,[2] Joseph Zabner,[2] and Michael J. Welsh[1,2,3]
[1]Howard Hughes Medical Institute
[2]Department of Internal Medicine
[3]Department of Physiology and Biophysics
University of Iowa College of Medicine
Iowa City, Iowa 52242
[4]Biology Department
Brookhaven National Laboratory
Upton, New York 11973

Summary

Adenovirus binds its receptor (CAR), enters cells, and replicates. It must then escape to the environment to infect a new host. We found that following infection, human airway epithelia first released adenovirus to the basolateral surface. Virus then traveled between epithelial cells to emerge on the apical surface. Adenovirus fiber protein, which is produced during viral replication, facilitated apical escape. Fiber binds CAR, which sits on the basolateral membrane where it maintains tight junction integrity. When fiber bound CAR, it disrupted junctional integrity, allowing virus to filter between the cells and emerge apically. Thus, adenovirus exploits its receptor for two important but distinct steps in its life cycle: entry into host cells and escape across epithelial barriers to the environment.

Introduction

Many viruses infect epithelia exposed to the external environment. During its life cycle, the virus must enter a cell, replicate, and then exit to infect a new host. In contrast to knowledge about viral entry and replication, much less is known about how viruses escape to the environment (Compans, 1995). Some enveloped viruses, such as influenza, bud from the epithelial cell's apical membrane, thereby escaping directly onto the mucosal surface (Rodriquez-Boulan and Sabatini, 1978). However, for viruses that do not use this strategy, we know little about how they cross physical barriers such as those presented by an epithelium.

Identification of viral receptors has yielded insight into mechanisms of viral entry (Baranowski et al., 2001; Compans, 1995; Schneider-Schaulies, 2000). In several cases, these receptors have turned out to be cell-cell adhesion proteins. Examples from viruses that infect epithelia include: coxsackie B viruses and adenoviruses 2 and 5 which bind to the coxsackievirus and adenovirus receptor (CAR; Bergelson et al., 1997), reoviruses which bind to the junctional adhesion molecule (JAM; Barton et al., 2001), rhinoviruses which bind to the intercellular adhesion molecule (ICAM-1; Greve et al., 1989; Staunton et al., 1989), and alphaherpesviruses which bind to the poliovirus receptor-related protein 1 (Prr1; Geraghty et al., 1998). However, it is not clear why viruses would utilize cell-cell adhesion molecules as receptors (Baranowski et al., 2001; White and Littman, 1989).

In fact, the discovery that some epithelia-tropic viruses use cell-cell adhesion molecules as receptors seemed surprising. When a virus approaches an epithelium from the apical surface, its receptor is hidden beneath the tight junctions on the basolateral membrane. Thus, with the normal portal of viral entry, the receptors are not readily accessible. This fact became readily apparent during attempts to develop gene transfer to differentiated airway epithelia for the genetic disease cystic fibrosis (Welsh, 1999). Attempts to deliver CFTR cDNA to a significant percentage of airway cells using recombinant adenoviruses 2 and 5, adeno-associated virus 2, and VSV-G pseudotyped retrovirus vectors all proved to be inefficient because airway epithelia segregate their receptors to the basolateral surface making them inaccessible to apically applied vector (Duan et al., 1998; Pickles et al., 1998; Walters et al., 1999; Wang et al., 1998; Zabner et al., 1997). In contrast to gene therapy applications, which use nonreplicating viral vectors, wild-type infection requires viral particles to enter only a few epithelial cells because subsequent replication expands their numbers. For viruses that utilize basolateral receptors, transient breaks in epithelial integrity likely provide virus with initial access to its receptor.

Thus, the observation that some epithelia-tropic viruses utilize basolateral cell-cell adhesion molecules as receptors raised the question of whether viruses might use these proteins for additional aspects of their life cycle. To explore this issue, we studied adenovirus 2, a nonenveloped virus that is released from infected cells during apoptosis (Horwitz, 1990). The receptor for adenovirus 2 is CAR, a member of the immunoglobulin receptor superfamily (Bergelson et al., 1997); it contains two extracellular Ig-like domains (D1 and D2). Structural and functional studies have shown that the D1 domain forms homodimers between molecules located on adjacent cells (van Raaij et al., 2000). Through this interaction, CAR serves as a cell-cell adhesion molecule (Honda et al., 2000). Consistent with this, CAR overexpression in airway epithelia increases transepithelial electrical resistance (Cohen et al., 2001). Fiber, and specifically its knob domain, is the adenovirus capsid protein that binds CAR (Bergelson et al., 1997; Freimuth et al., 1999; Henry et al., 1994; Louis et al., 1994). A crystal structure of fiber-knob bound to CAR revealed that the fiber-knob:CAR interface overlaps with the CAR:CAR interface involved in dimer formation (Bewley et al., 1999; van Raaij et al., 2000). Moreover, fiber-knob binds CAR with a higher affinity than CAR binds to itself (Freimuth et al., 1999; van Raaij et al., 2000). These observations suggested that fiber-knob might competitively inhibit CAR:CAR dimer formation.

After a virus enters a cell and replicates, the role, if any, of interactions between adenovirus fiber and CAR are uncertain. It is well known that during an infection with adenovirus 2 and 5, cells produce fiber protein in

Correspondence: michael-welsh@uiowa.edu

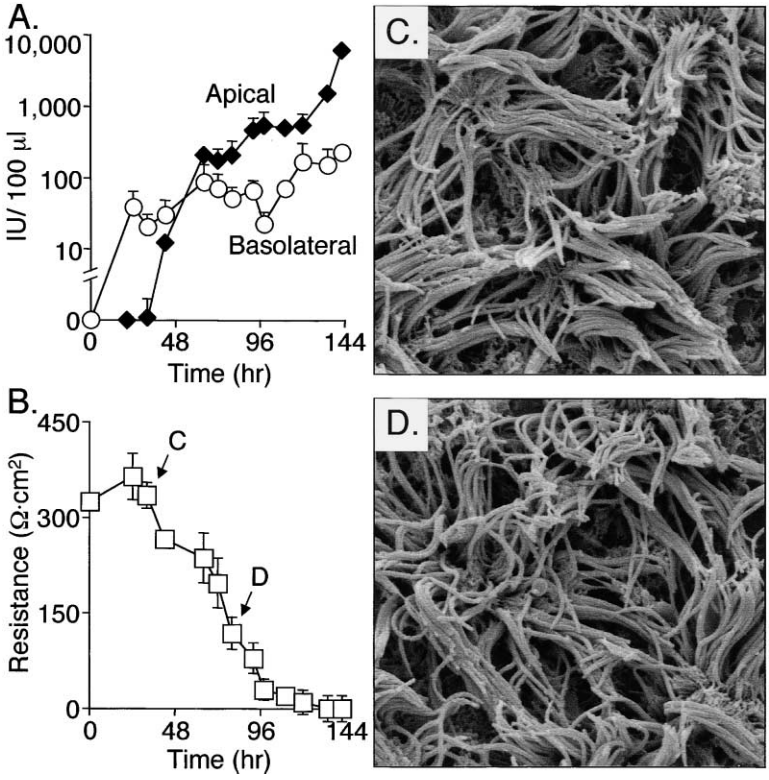

Figure 1. Viral Release and Epithelial Integrity during Wild-Type Infection of Well-Differentiated Human Airway Epithelia

(A) Amount of adenovirus released to the apical (◆) or basolateral (○) side of epithelia infected from the basolateral surface with adenovirus 2 at time zero. Data are plotted as a function of time postinfection. Data are mean ± SEM of viral titers for 6 experiments. (B) Transepithelial electrical resistance (Rt) (□) is shown for the infected epithelia in (A). (C and D) Scanning electron photomicrographs of the apical surface of infected epithelia at 36 hr (C) and 68 hr (D) postinfection; time points at which microscopy was performed are indicated in (B).

substantial excess of what is incorporated into the virion (Boulanger and Puvion, 1973; Huebner et al., 1954). Fiber is also present on defective viral particles, which are produced in large excess of infectious virions for adenovirus as well as most other animal viruses. Previous studies have also shown that exogenous fiber protein competes for CAR and prevents adenovirus binding and infection (Freimuth et al., 1999; Santis et al., 1999). Thus, production of excess fiber protein might seem counterproductive because it could block adenovirus spread.

Based on all these observations, we speculated that adenovirus might exploit fiber-CAR interactions not solely to enter cells, but also to cross tissue barriers. We hypothesized that adenovirus fiber protein interrupts cell-cell adhesion, making it possible for the virus to escape across the airway epithelium. This process could facilitate viral shedding with subsequent spread to distal sites in the epithelium and to another host.

Results

Adenovirus Escape to the Apical Surface of Airway Epithelia through the Paracellular Pathway

For these studies, we used an airway model consisting of primary cultures of human airway epithelia grown at the air-liquid interface (Karp et al., 2002). These epithelia develop tight junctions, a barrier to transepithelial particle and solute movement, and a well-differentiated morphology consisting of a pseudostratified columnar epithelium with ciliated, goblet, and basal cells. Thus, they closely resemble the in vivo human airway. In these epithelia, CAR is localized on basal cells, where it is most highly expressed, and on the basolateral membrane of columnar cells abutting the airway lumen (Walters et al., 1999).

To investigate virus escape from the epithelium, we examined the polarity of wild-type adenovirus 2 release following infection from the basolateral surface (Figure 1A). Initially following infection, progeny virus was released only to the basolateral surface. After a short delay, virus then appeared on the apical surface. Coincident with virus escape to the airway lumen, transepithelial electrical resistance (Rt) fell (Figure 1B). Although Rt fell, scanning electron microscopy revealed no change in morphology of the apical surface, which was covered by ciliated cells and interspersed goblet cells (Figures 1C and 1D). These data suggested that early after infection, adenovirus might escape to the apical surface by traveling between the cells through the paracellular pathway.

This conclusion was supported by transmission electron microscopy, which revealed adenovirus-infected basal cells undergoing apoptotic cell death; they had membrane blebs, mitochondrial breakdown, and condensed cytoplasm (note cell marked with asterisk in Figure 2A). These cells were filled with viral particles (inset of Figure 2A). In addition, we observed virus outside infected cells in the paracellular space. Away from virus-producing basal cells, the paracellular pathway showed a tightly interdigitated space and closely apposed cell membranes, and we saw no adenovirus particles between cells (Figure 2B). However, close to and directly above infected cells, the cell-cell junctions were discontinuous and there were small gaps between the columnar cells (Figure 2C). Within these gaps, adenovirus particles extended up toward the apical surface.

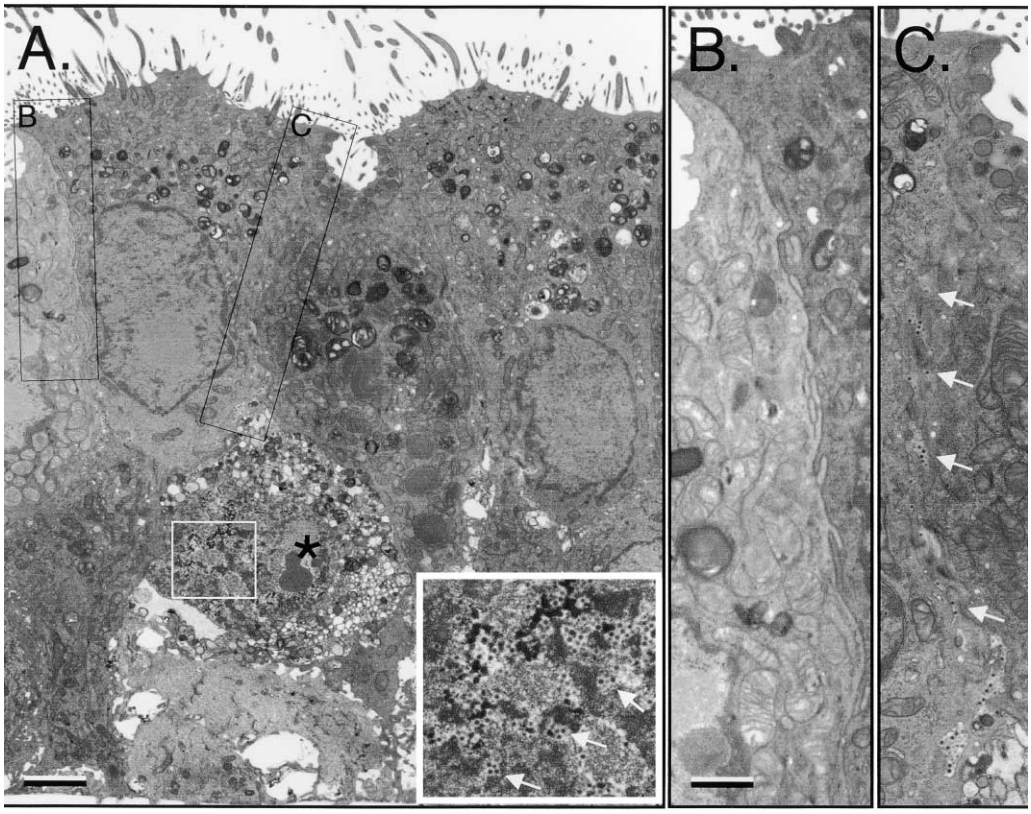

Figure 2. Transmission Electron Photomicrographs of Adenovirus-Infected Epithelium Showing Adenovirus in the Paracellular Space

(A) Example of epithelia studied 68 hr postinfection (same epithelium as shown in Figure 1D). Asterisk indicates adenovirus infected basal cell. Inset shows a magnified field from the nucleus of the infected cell. White arrows indicate adenovirus particles in the infected cell. Black boxes indicate the regions magnified in (B) and (C). Bar represents 5 μm.

(B and C) Magnification of columnar cell-cell junction at a site distant from the infected cell (B), or directly above the infected cell (C). White arrows indicate adenovirus particles between two columnar cells. Bar indicates 15 μm for (B) and (C).

Thus, early in the course of infection, adenovirus released from basal cells spread through the paracellular space toward the apical surface. These findings suggested that adenovirus might interrupt epithelial cell-cell contacts to gain access to the airway lumen, and hence the environment.

Basolateral Fiber-Knob Protein Increased Epithelial Permeability

Previous reports indicated that adenovirus 2 and 5-infected cells produce much more fiber protein than is incorporated into adenovirus particles (Boulanger and Puvion, 1973; Huebner et al., 1954). In addition, fiber is present on defective particles, which exist in excess of infectious virions. To determine if infected airway epithelia produce fiber in excess of another capsid protein, we compared the ratio of fiber to hexon in the lysate of infected epithelia to that in viral particles purified to remove unincorporated proteins. The level of fiber relative to hexon was greater in lysate than in purified viral particles (Figure 3A). Hence, infected airway epithelia generated fiber in excess of that contained in virions.

We hypothesized that fiber protein might block CAR-mediated cell-cell contacts and increase paracellular permeability. To test this, we added recombinant fiber-knob to the basolateral surface and found that it reduced Rt (Figure 3B). When fiber-knob was removed, Rt returned to basal values. These data indicated that fiber-knob elevated epithelial permeability, probably by increasing paracellular permeability, and that the effect was reversible. If we mixed fiber-knob with the soluble extracellular D1 domain of CAR (sCAR) before adding it to the epithelium, the reduction in Rt was significantly attenuated (Figure 3B). This result suggested it is the binding of fiber-knob to CAR on the cell surface that increases epithelial permeability. Since CAR is located on the basolateral membrane (Pickles et al., 1998; Walters et al., 1999), we predicted that adding fiber-knob to the apical surface would have no effect on epithelial permeability. Figure 3B shows that apical fiber-knob failed to alter Rt.

The fiber-induced increase in ionic permeability (reduction in Rt) suggested that epithelial permeability to adenovirus might also increase. To test this prediction, we added recombinant, replication-defective adenovirus to the basolateral surface of fiber-knob pretreated epithelia maintained at 15°C and measured its appearance in the apical fluid (Figure 3C). With basolateral fiber-knob pretreatment, the virus filtered through the epithelium to appear on the apical surface. This permeability was partially blocked when fiber-knob was complexed with sCAR. In addition, adenovirus did not cross

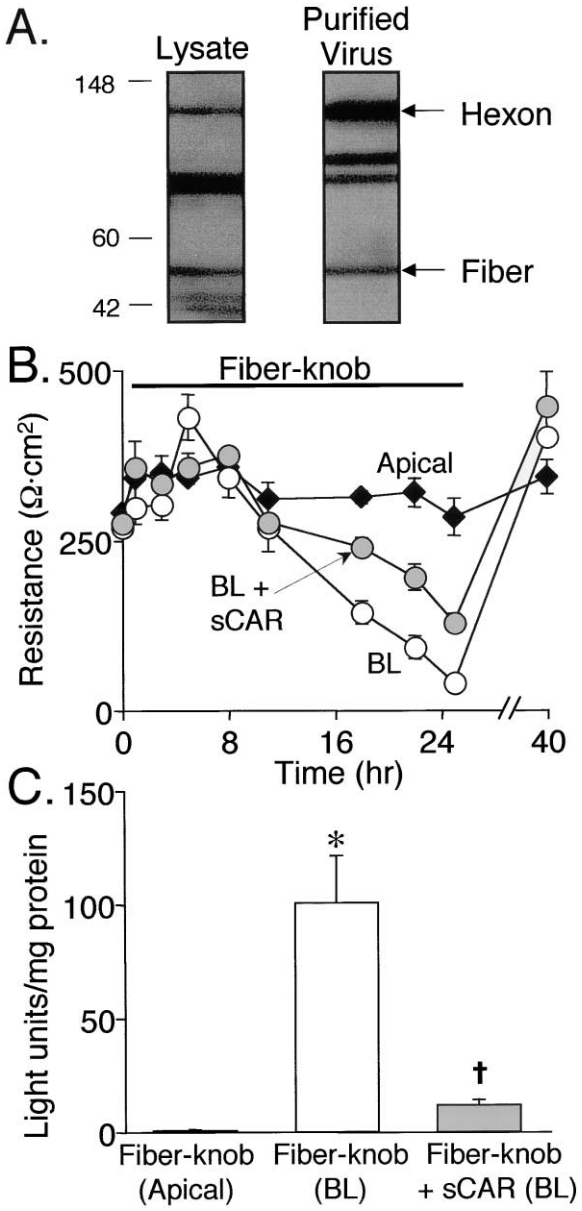

Figure 3. Fiber Production and the Effect of Fiber-Knob on Rt and Adenovirus Permeability

(A) Lysate from adenovirus-infected epithelia and purified adenoviral particles blotted with human anti-adenovirus serum that recognizes all viral proteins. Migration of hexon and fiber are indicated. Additional bands are either adenoviral proteins not detected in lysate, or nonspecific proteins from epithelia recognized by human anti-adenovirus serum.

(B) Rt across well-differentiated epithelia treated with recombinant fiber-knob either on the apical side (◆), basolateral side (○), or basolateral side in the presence of sCAR (shaded circle). sCAR was mixed with fiber-knob in a 1:1 molar ratio. Fiber-knob was present during the time indicated by the bar. $n = 6$.

(C) Adenovirus movement from the basolateral to the apical surface of epithelia following pretreatment with fiber-knob. The amount of recombinant virus encoding β-galactosidase collected from the apical surface was assessed by applying the collected liquid to 293 cells and measuring β-galactosidase activity 24 hr later (as light units). Asterisk indicates $p < 0.05$ compared to apical fiber-knob and cross indicates $p < 0.05$ compared to basolateral fiber-knob. $n = 6$.

epithelia pretreated with apical fiber-knob (Figure 3C). Similar results were obtained when we applied virus to the apical surface and measured its appearance in the basolateral liquid (data not shown). These results indicate that fiber-knob binds CAR and increases bidirectional epithelial permeability to ions and to adenovirus particles.

To probe further the mechanism of fiber-mediated changes in Rt, we examined epithelial architecture and the structures that maintain epithelial tight junctions and adherens junctions. Immediately after adding basolateral fiber, epithelia were intact with tightly opposed cell-cell contacts (Figure 4A). ZO-1 was localized at the apex of cell-cell contacts, and β-catenin resided below ZO-1 on the upper portion of the lateral cell membrane (Figure 4D). After a delay, fiber caused separation of cell-cell contacts and spaces appeared between the cells (Figure 4B). This coincided with a redistribution of β-catenin to a more basal location, although ZO-1 remained primarily at the apex of cell-cell contacts (Figure 4E). Prolonged incubation with fiber eventually disrupted cell-cell contacts at the apex of the cell, including the area of the tight junctions (Figure 4C). This was supported by the circumferential redistribution of β-catenin and the loss of discrete ZO-1 staining (Figure 4F).

CAR Lies Below the Tight Junctions and Maintains the Epithelial Barrier

Previous work suggested that CAR can form homotypic cell-cell interactions, predicting it might contribute to the epithelial barrier (Cohen et al., 2001; Honda et al., 2000). However, the understanding of the role played by CAR in epithelia is limited. To examine the subcellular localization of CAR, we expressed a flag-tagged CAR in well-differentiated human airway epithelia. CAR was present in the cytoplasm and concentrated on the plasma membrane (Figure 5A). Cell-surface staining of CAR overlapped with that of the adherens junction protein β-catenin. In cells stained for the cytoplasmic tight junction-associated protein ZO-1 and examined with confocal microscopy, CAR staining appeared just below that of ZO-1 (Figures 5B–5D). This pattern was readily appreciated in optical sections taken at the intersection of the tight junction and the adherens junction (Figure 5B). In optical sections just above this region (i.e., at the tight junction level), ZO-1 was observed but not CAR (Figure 5C); just below this region (i.e., at the adherens junction level), ZO-1 staining was absent and CAR staining appeared (Figure 5D).

Immunoprecipitation of the adherens junction protein β-catenin from epithelial cell lysates coprecipitated CAR (Figure 5E). Likewise, CAR coimmunoprecipitated β-catenin (Figure 5F). These data suggest that CAR is a molecular component of the apical junctional complex, and specifically, it lies just below the tight junction in the adherens junction. We do not know how CAR interacts with β-catenin. However, a recent crystal structure has shown how β-catenin interacts with another adherens junction protein, E-cadherin (Huber and Weis, 2001). Interestingly, approximately 40% of the E-cadherin residues involved in the interaction share homology with CAR, suggesting that a similar region in E-cadherin and CAR bind to β-catenin. These observations sug-

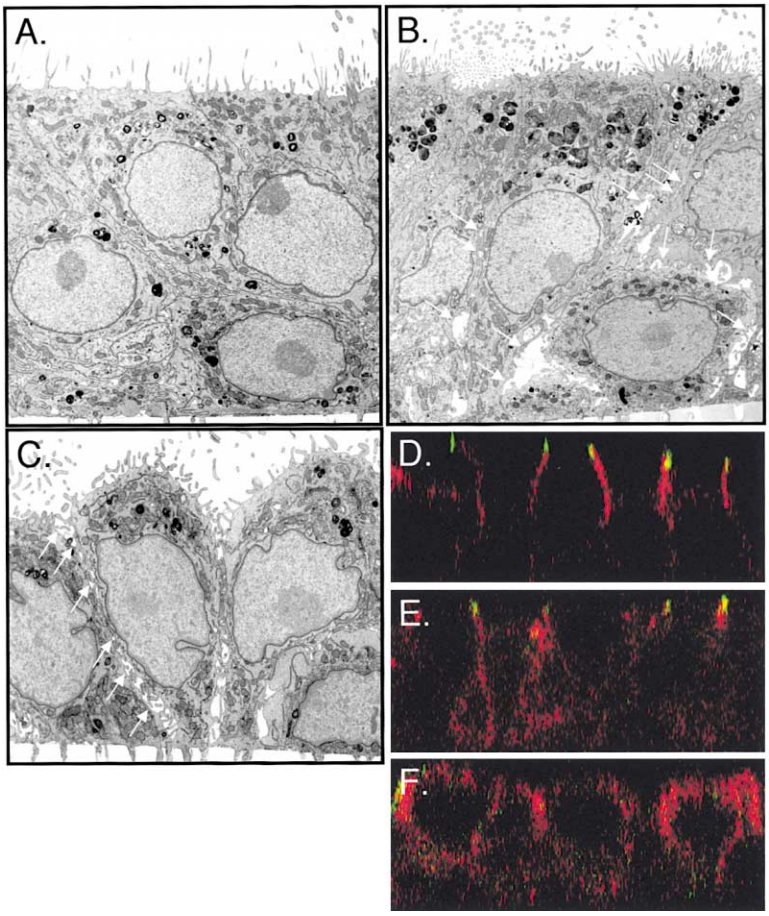

Figure 4. Effect of Fiber on Epithelial Morphology and Molecular Architecture of the Apical Junction Complex

(A–C) Transmission electron photomicrographs of epithelia studied immediately after (A), 20 hr after (B), and 36 hr after (C) addition of fiber-knob.

(D–F) Immunocytochemistry of ZO-1 (green) and β-catenin (red) in epithelia studied immediately after (D), 20 hr after (E), and 36 hr after (F) addition of fiber-knob. Arrows indicate loss of tight apposition of cell membranes.

gested that β-catenin might bind CAR or E-cadherin, but probably not both simultaneously. Consistent with this speculation, we found that CAR did not coimmunoprecipitate E-cadherin (data not shown).

The location of CAR and our data with fiber-knob addition suggested that CAR has an important functional role in the epithelial barrier. To test this, we overexpressed CAR in airway epithelia and measured Rt. Increasing CAR expression increased basal Rt (Figure 6A), consistent with previous data (Cohen et al., 2001). Conversely, blocking CAR by adding an anti-CAR antibody to the basolateral solution significantly reduced Rt (Figure 6B). When the antibody was removed, Rt recovered. Apical anti-CAR antibody had no effect, consistent with the conclusion that CAR lies beneath the tight junction seal where it is inaccessible from the apical surface. The anti-CAR antibody also inhibited recovery of Rt following Ca^{2+} chelation (Figure 6C) and retarded the development of Rt in freshly seeded cells (Figure 6D). These results indicate that CAR is required for establishing and maintaining the airway epithelial barrier. They also position CAR beneath the tight junction seal.

The D1 domain of CAR forms homodimers, and it binds fiber-knob (Bergelson et al., 1997; Freimuth et al., 1999; van Raaij et al., 2000). When we added soluble D1 domain (sCAR) to the basolateral surface of differentiated epithelia, Rt decreased (Figure 6E). Removing the protein reversed this effect. In contrast, apical sCAR did not change Rt. These data indicate that the function of CAR in epithelial cell-cell adhesion involves the D1 domain, i.e., the domain that also binds fiber-knob. CAR's cell-cell adhesion function might require other cell adhesion molecules of the adherens junctions, such as E-cadherin. To test this possibility, we studied A549 cell-cell association in the presence of soluble D1 domain to block CAR association and in the absence of Ca^{2+} to block E-cadherin association. Either intervention alone partially blocked cell-cell association, and the combination completely disrupted cell-cell adhesion (data not shown). Thus, CAR appears to function independently of cadherin.

Adenovirus Escape to the Apical Surface Requires a Fiber-Knob-Mediated Increase in Airway Epithelial Permeability

These results raised the question of whether fiber is required for adenovirus to increase paracellular permeability and escape to the apical surface. To answer this question, we infected differentiated epithelia with wild-type adenovirus. After a period of stability, Rt fell in control epithelia, indicating a significant increase in paracellular permeability (Figure 6G). In a second group of epithelia, once Rt began to fall (72 hr postinfection), we added neutralizing anti-adenovirus serum; the serum contained antibodies directed against many viral proteins including fiber (Figure 6F). As a result, Rt stabilized (Figure 6G). This rapid effect further supports the conclusion that the initial decrease in Rt resulted from an in-

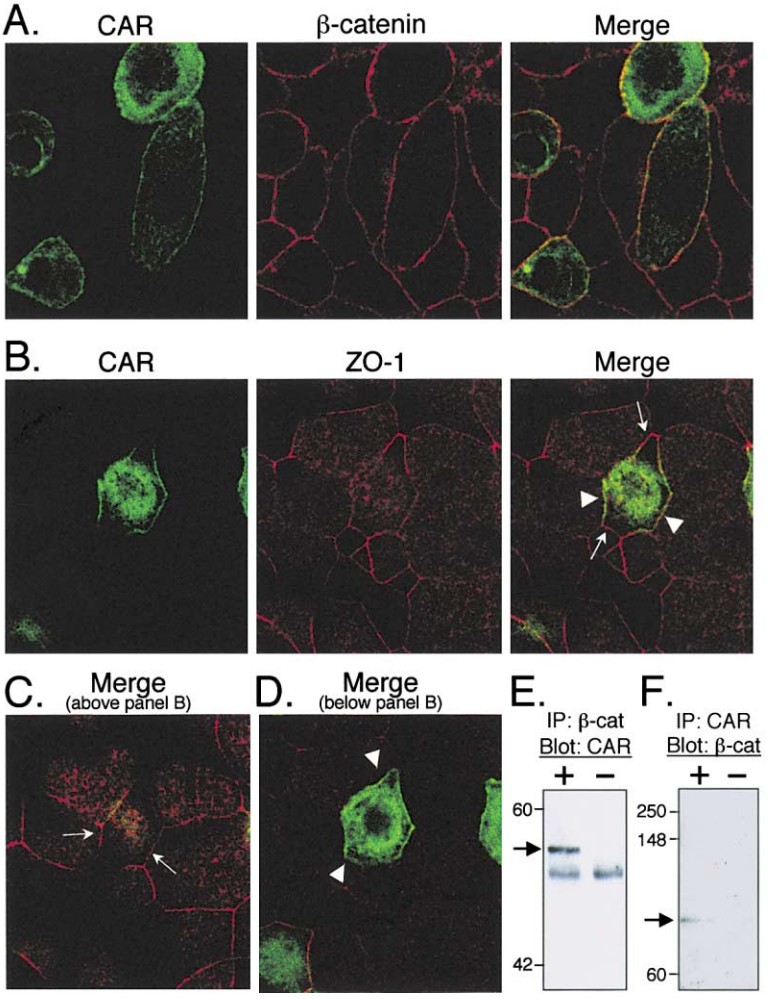

Figure 5. Localization and Molecular Interactions of hCAR Assessed by Immunocytochemistry and Immunoprecipitation

(A) Immunocytochemistry of hCAR (green) and β-catenin (red) in well-differentiated human airway epithelia. CAR expressing cells are indicated by green staining in the cytoplasm.

(B–D) Immunocytochemistry of hCAR (green) and ZO-1 (red) in airway epithelia around the area of the tight junction. (B) shows a confocal section taken at the intersection of the tight junction (arrow) and the adherens junction (arrowhead). The plane of (C) is at the level of the tight junction and immediately above that in (B). The plane of (D) is immediately below that of (B), at the level of the adherens junction.

(E and F) Coimmunoprecipitation of CAR and β-catenin: lysate from A549 cells precipitated with anti-β-catenin and blotted for CAR (E), or precipitated with anti-CAR and blotted with anti-β-catenin (F). "+" and "−" indicate presence and absence of precipitating antibody, respectively. Arrow in (E) indicates CAR, and lower band is immunoglobulin. Arrow in (F) indicates β-catenin. Molecular weight standards are shown on the left of each panel.

crease in paracellular permeability rather than cell death or lysis. To determine whether the effect was due to the anti-fiber activity, we applied the same serum after anti-fiber antibodies had been depleted. Depletion of anti-fiber activity did not remove antibodies to other adenovirus proteins (Figure 6F) or reduce the neutralizing activity of the serum (Experimental Procedures). Without anti-fiber activity, Rt continued to fall (Figure 6G).

We also measured escape of adenovirus onto the apical surface. Serum with anti-fiber activity inhibited apical shedding (Figure 6H). Moreover, inhibition of apical release was dependent on anti-fiber activity. These data indicate that fiber-CAR interactions are both sufficient and required for an increase in epithelial permeability and adenovirus movement across the epithelial barrier.

Discussion

These results suggest a model of CAR function and its role in adenovirus escape from the epithelium (Figure 7). CAR resides in basal cells and in columnar cells, where it lies just beneath the tight junction seal in adherens junctions. In columnar cells, it serves as a cell-cell adhesion molecule maintaining the apical junction complex (Figure 7, left). Because CAR is normally inaccessible from the apical surface, the initial adenovirus infection may occur when a transient break in the epithelium allows luminal virus to reach its receptor or during the repair of injured epithelium when CAR might be accessible. Following viral replication, infected cells release both infectious and defective viral particles, as well as excess free fiber protein (Figure 7, right). Fiber from defective particles or free protein binds CAR, interrupting adherens junction cell-cell contacts and thereby increasing epithelial permeability. Fiber-CAR interactions out compete CAR-CAR interactions because fiber has a higher binding affinity for CAR (Freimuth et al., 1999; van Raaij et al., 2000), and there is likely an excess molar ratio of fiber to CAR. Because the paracellular pathway is made leaky, adenovirus particles filter between the epithelial cells to emerge on the apical surface where they can spread either to a new host or to other regions of the lung. Free fiber or fiber on defective particles may further facilitate adenovirus escape by blocking infectious virus binding to receptors on adjacent cells; as a result more of the virus would be available to diffuse to the apical surface. Such fiber-dependent blocking of the adenovirus receptor would be somewhat analogous to the role of neuraminidase in influenza in-

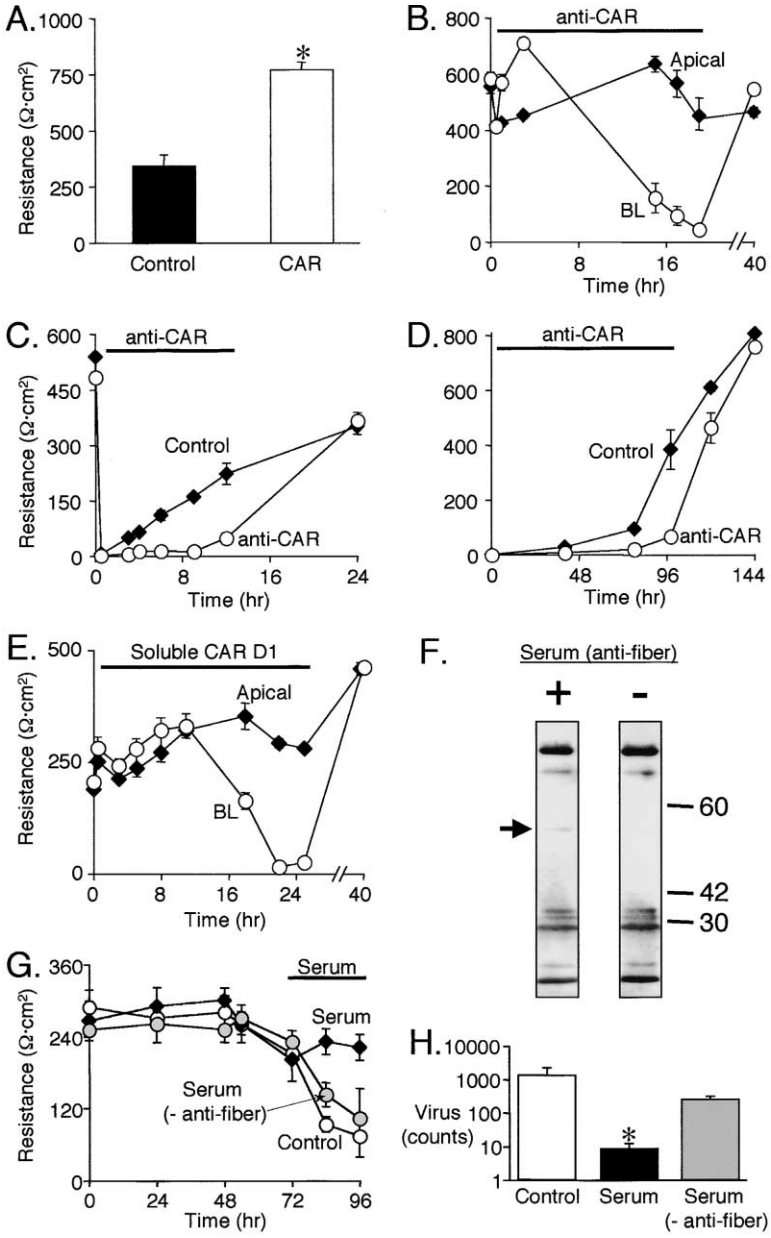

Figure 6. Effect of Increasing CAR Expression and Blocking CAR on Rt, and Effect of Serum with and without Anti-Fiber Activity on Wild-Type Adenovirus Release from Well-Differentiated Human Airway Epithelia

(A) Steady-state Rt in well-differentiated human airway epithelia in control epithelia and epithelia overexpressing CAR. Data for (A–E) are mean ± SEM Rt for 6 experiments. Asterisk indicates $p < 0.05$.

(B) Transepithelial resistance in differentiated epithelia treated with anti-CAR antibody either on the apical side (◆) or the basolateral side (○). Treatments for (B–E) were present during times indicated by the bars.

(C) Time-course of recovery of Rt after Ca^{2+} chelation in the presence of anti-CAR (○) or a control antibody (◆).

(D) Development of Rt in freshly seeded cells treated with anti-CAR (○) or control antibody (◆).

(E) Steady-state Rt in epithelia treated with sCAR either on the apical side (◆) or the basolateral side (○).

(F) Denatured adenovirus particles blotted with serum (+) or serum depleted of anti-fiber activity (−). Arrow indicates fiber.

(G) Rt of infected epithelia treated with serum (◆), serum depleted of anti-fiber activity (shaded circle), or vehicle control (○). Serum was present during time indicated by bar. n = 6.

(H) Amount of adenovirus released to the apical side at 84 hr after infection. Asterisk indicates $p < 0.05$ compared to control. n = 6.

fection; neuraminidase cleaves the influenza receptor from the cell surface thereby preventing virus binding and allowing influenza virus escape to the environment (Hirst, 1950). It is interesting that the common clinical isolates of adenovirus (i.e., serotypes 2 and 5) make more fiber protein than other less common isolates (i.e., serotype 12) (P.F., unpublished data). We speculate that this difference might play a role in the pathogenesis of infection.

The fiber-CAR interaction might also be important in systemic spread of the virus. For example, CAR is expressed on endothelial cells (Carson et al., 1999), and disruption of CAR-mediated endothelial cell-cell adhesion could facilitate spread to the bloodstream. From the bloodstream, virus could travel to other sites in the body.

A recent study showing CAR and ZO-1 staining in a similar location and coimmunoprecipitation of the two proteins suggested that CAR is a component of the apical junction complex (Cohen et al., 2001). This complex is formed by interactions of adherens junction proteins (e.g., β-catenin) and tight junction proteins (e.g., ZO-1) (Rajasekaran et al., 1996). Specifically, the adherens junction acts as a scaffold for the tight junction, i.e., tight junctions fall apart with disruption of the adherens junction (Gumbiner, 1996). Our current data are consistent with these studies and extend them to further position CAR in cell-cell junctions and identify its contribution to tight junction function. Our immunocytochemical labeling indicated that CAR sits immediately below ZO-1 where it associated with β-catenin and contributed to the epithelial barrier. This location was further supported by our functional data showing that fiber-knob, anti-CAR antibody, and the CAR D1 domain could ac-

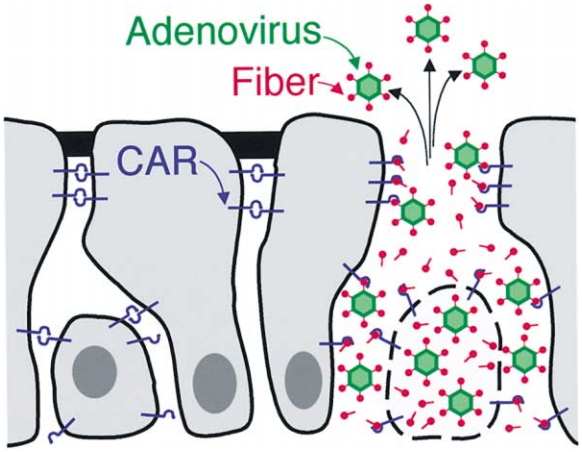

Figure 7. Model of Adenovirus Escape from Airway Epithelia

Epithelial cells sequester CAR (blue) on the basolateral membrane below the level of the tight junction seal and on basal cells. Once infection is established, virus and fiber protein (red) are released basolaterally. Fiber increases paracellular permeability by competing CAR-mediated cell-cell adhesion. This allows adenovirus escape to the apical surface.

cess CAR only from the basolateral surface, not from the apical surface. If CAR were a part of the tight junction seal, it should have been accessible from either surface. Previous studies indicate that claudins and occludins form the tight junction seal, distinguishing the size and selectivity of permeating substances (Tsukita et al., 2001). CAR appears to hold the cell membranes in close apposition so that the seal can be maintained. Given the sequence similarity to CAR, it is interesting that JAM seems to perform a similar function in epithelial cell-cell adhesion (Itoh et al., 2001; Liang et al., 2000). However, CAR did not coimmunoprecipitate JAM (data not shown).

Adenoviruses also utilize other mechanisms to escape into the environment. For example, very late in the course of infection, cell death and sloughing occur (Horwitz, 1990); this will spill adenovirus particles into the airway lumen. However, the reversible increase in paracellular permeability we report here provides a mechanism for virus shedding and spread early after an infection, perhaps before the development of a neutralizing antibody response. While our findings may be explained by mechanical blocking of CAR-CAR interactions by basolateral fiber, we cannot exclude the possibility that fiber binding to CAR triggers an intracellular signaling cascade that contributes to the increased epithelial permeability. It is also possible that adenovirus penton base, which binds basolateral integrins, might facilitate adenovirus movement across epithelial barriers.

Some other viruses also utilize basolateral cell-cell adhesion molecules as receptors (Barton et al., 2001; Geraghty et al., 1998; Greve et al., 1989; Staunton et al., 1989). Our data suggest that perhaps like adenovirus, some of them might usurp the receptor's normal function in cell-cell adhesion to loosen the paracellular path and thereby facilitate spread to other compartments including the environment. In this regard, reoviruses are particularly interesting because they use JAM, a receptor related to CAR (Barton et al., 2001). Viruses have also used basolateral receptors for other purposes. For example, binding of reovirus σ1 to its receptor JAM stimulates NF-κB-induced apoptosis, which might minimize tissue inflammation and downregulate the immune response (Barton et al., 2001; Teodoro and Branton, 1997). Thus, understanding the multiple consequences of the interaction between a virus and its receptor may improve understanding of viral pathogenesis, including tissue invasion and host-host transmission.

Our data indicate that adenovirus uses the same molecules, fiber and CAR, for two different purposes. To initiate infection, the interaction of fiber with CAR is key to cell binding and entry of the virus (Bergelson et al., 1997). Then following replication, the interaction of fiber with CAR competes CAR-CAR homodimers that mediate cell-cell adhesion. This allows the virus to cross tissue barriers so that it can spread to new compartments including the environment. Thus, this interaction apparently evolved to serve two equally important, yet fundamentally different steps in the adenovirus life cycle.

Experimental Procedures

Epithelial and Cell Culture

Airway epithelial cells were obtained from trachea and bronchi of lungs removed for donation. Cells were isolated by enzyme digestion as previously described (Karp et al., 2002). Freshly isolated cells were seeded at a density of 5×10^5 cells/cm^2 onto collagen-coated, 0.6 cm^2-area Millicell polycarbonate filters (Millipore Corp., Bedford, MA). The cells were maintained at 37°C in a humidified atmosphere of 5% CO_2 and air. Twenty-four hours after plating, the mucosal media was removed and the cells were allowed to grow at the air-liquid interface. The culture media consisted of a 1:1 mix of DMEM/Ham's F12, 5% Ultraser G (Biosepra SA, Cergy-Saint-Christophe, France), 100 U/ml penicillin, 100 μg/ml streptomycin, 1% nonessential amino acids, and 0.12 U/ml insulin. Airway epithelia first reached confluence and developed a transepithelial electrical resistance, indicating the development of tight junctions and an intact barrier. Then they were cultured at least 14 days after seeding during which time they differentiated and developed a ciliated surface as assessed by scanning electron microscopy (Karp et al., 2002; Zabner et al., 1996).

A549 cells were cultured on 100 mm plates (Corning Costar, Corning, NY) in a 1:1 mix of DMEM/Ham's F12 (Sigma Chemical Co., St. Louis, MO) supplemented with 10% fetal calf serum (Sigma Chemical Co.), 1% nonessential amino acids, 100 U/ml penicillin, and 100 μg/ml streptomycin.

Viruses, Recombinant Proteins, and Antibodies

Wild-type adenovirus serotype 2 (Ad2/wild-type) and recombinant adenovirus expressing β-galactosidase (Ad5/β-gal) or flag-tagged hCAR (Ad5/hCAR) were prepared by the University of Iowa Gene Transfer Vector Core at titers of approximately 10^{11} infectious units (IU)/ml for wild-type and 10^{10} IU/ml for recombinant virus.

Recombinant fiber-knob (type 2) with an N-terminal 6-His tag was expressed in bacteria and purified by metal affinity chromatography using standard procedures (Qiagen, Valencia, CA). Soluble D1 domain of CAR (sCAR) was expressed in bacteria and purifed with affinity chromatography. Briefly, purified fiber-knob was coupled to Sepharose beads (CNBr-activated) according to the manufacturer's instructions (Amersham Pharmacia Biotech, Piscataway, NJ). *E. coli* lysates containing sCAR were passed over the column, and the column was then washed with 10 mM Tris and 100 mM NaCl, at pH 8. Bound sCAR was eluted with low pH buffer (100 mM sodium acetate, [pH 4]). Eluate fractions were collected in tubes containing 1/10 fraction volume of 1 M Tris buffer, at pH 8.8 to neutralize the pH of the eluate. Peak fractions were pooled and dialyzed against PBS.

The hybridoma cell line for anti-CAR antibody (RcmB, American Type Culture Collection, Rockville, MD) was grown in CELLine CL-1000 flasks (Integra Biosciences) with CD hybridoma media (Invitrogen, Carlsbad, CA). Neutralizing serum was obtained from normal human subjects and depleted of anti-fiber activity. Briefly, fiber-knob was coupled to an Affi-gel 10 matrix according to the manufacturer's instructions (Bio-Rad, Hercules, CA). Neutralizing serum was then diluted 1:1 with PBS and incubated with the fiber-knob matrix for 4 hr at 4°C. The flowthrough from the column was collected and saved. The column was stripped of bound antibody by eluting with 50 mM glycine, 135 mM NaCl, at pH 2.5. Flowthrough was subjected to three rounds of purification and stored at 4°C. The neutralizing activity of serum and serum depleted of anti-fiber activity were not significantly different.

Adenovirus Infection

Well-differentiated human airway epithelia were infected with Ad2/wild-type by incubating 10 moi of virus in EMEM on the basolateral surface for 30 min at 37°C. Epithelia were then rinsed, refed, and maintained at the air-liquid interface at 37°C. To measure apical release of wild-type virus, a 100 μl aliquot of EMEM was added to the apical surface and sampled 30 min later. For basolateral release, a 100 μl sample of basolateral media was collected. Media was refreshed after each time point. Samples were then titered on 293 cells. Viral titers shown in Figure 1 represent release during the indicated interval. Titers were determined by fixing cells with acetone/methanol and staining with a polyclonal FITC-labeled anti-hexon antibody (Chemicon, Temecula, CA) 24 hr after infection. Hexon-positive cells were counted by fluorescence microscopy (Zabner et al., 1997). Transepithelial resistance was measured using an ohm meter (World Precision Instruments, Sarasota, FL). Excess fiber protein production was determined by comparing the ratio of fiber to hexon in purified virus particles versus the ratio in infected epithelia. Purified virus and epithelia were incubated at 4°C for 30 min with lysis buffer (1% Triton X-100, 10 mM Tris-HCl, [pH 7.4], and 150 mM NaCl), supplemented with protease inhibitors (10 μg/ml each of leupeptin, aprotinin, and pepstatin A). Samples were blotted with anti-adenovirus serum as described below. For studies with neutralizing serum, Ad2-infected epithelia were treated with a 2-fold dilution of serum or serum depleted of anti-fiber activity in PBS. Since serum treatments are predicted to neutralize the virus, apical release of virus was determined by dot blot of apical fluid.

Electron Microscopy

At various times after adenovirus infection, epithelia were fixed in 2.5% gluteraldehyde in 0.1 M sodium cacodylate at pH 7.2 and processed for scanning and transmission electron microscopy using standard procedures. Briefly, cultures destined for transmission microscopy (TEM) were postfixed in 1% osmium tetroxide, stained en bloc in 1% uranyl acetate, followed by dehydration in a graded series of ethanol. The samples were then transitioned to Eponate 12 (Ted Pella, Redding, CA), embedded and cured overnight at 65°C. Thin sections were cut at 80 nm and picked up on 200-mesh copper grids. Grids were poststained with Reynold's lead citrate and 5% uranyl acetate. The sections were examined on a Hitachi H-7000 TEM. Following dehydration, samples for scanning electron microscopy (SEM) were rinsed twice in hexamethyldisilazane, air dried, and mounted on aluminum stubs with colloidal silver paint. The filters were sputter-coated with 60:40 gold-palladium and imaged on a Hitachi S-4000 field emission SEM.

Fiber-Knob, CAR, and Epithelial Permeability

Fiber-knob was added to the apical or basolateral surface of epithelia at 0.2 mg/ml at 37°C. For the fiber-knob:sCAR condition, stoichiometric amounts of protein (1:1 molar ratio, 0.07 mg/ml sCAR) were incubated for 1 hr at 37°C prior to treating epithelia. Transepithelial resistance was measured as above. Adenovirus permeability was determined by adding Ad5/β-gal at 1×10^9 IU/ml to the basolateral surface of inverted epithelial cultures for 2 hr at 15°C. The apical surface was then washed for 10 min with EMEM; the solution was then added to 293 cells for 1 hr at 37°C. Twenty-four hrs later, total β-galactosidase activity was measured using a commercially available method (Galacto-Light, Tropix Inc., Bedford, MA). After rinsing with PBS, cells were incubated with 120 μl lysis buffer (25 mM Tris-phosphate, [pH 7.8]; 2 mM DTT; 2 mM 1, 2-diaminocyclohexane-N,N,N',N'-tetraacetic acid; 10% glycerol; and 1% Triton X-100) for 30 min. Light emission was quantified in a luminometer (Analytical Luminescence Laboratory, San Diego, CA).

To increase CAR expression, epithelia were incubated with 50 moi of Ad5/hCAR or Ad5/β-gal (as a control) on the basolateral surface for 30 min at 37°C (van't Hof and Crystal, 2001). Rt was measured 48 hr later. To disrupt tight junctions, epithelia were treated with 8 mM EGTA added to the apical and basolateral surface in EMEM for 30 min at 37°C to chelate Ca^{2+}, rinsed with EMEM, and Rt was measured during reformation of the tight junctions. In experiments designed to block endogenous CAR, differentiated epithelia were treated with anti-CAR antibody at 30 μg/ml in CD hybridoma media either on the apical or the basolateral side at 37°C. For studies using Ca^{2+} chelation or assessing development of Rt, epithelia were treated with anti-CAR antibody (30 μg/ml) or anti-flag antibody as a control (Sigma Chemical Co.). Antibody was added immediately after EGTA was removed or 1 day postseeding. To study the effect of sCAR on differentiated epithelia, protein was added apically or basolaterally at 0.2 mg/ml in EMEM.

Immunocytochemistry, Immunoprecipitation, Western and Dot Blots

Immunocytochemistry was performed on well-differentiated human airway epithelia expressing flag-tagged hCAR as described in the preceding paragraph. Briefly, epithelia were fixed with 4% paraformaldehyde for 15 min at 20°C. Unless otherwise noted, SuperBlock (Pierce, Rockford, IL) was used to wash between incubations and to dilute reagents. Epithelia were rinsed, permeabilized with 0.2% Triton X-100 for 15 min, and washed twice, 10 min each. Mouse anti-Flag monoclonal antibody (1:500; Sigma Chemical Co.) and either rabbit anti-β-catenin or rabbit anti-ZO-1 antibodies (both at 1:100; Zymed, San Francisco, CA) were added for 1 hr at 37°C. Cells were then rinsed twice for 10 min each and incubated with goat α-mouse IgG conjugated with Alexa 488 fluorophore and goat α-rabbit IgG conjugated with Alexa 568 fluorophore (both at 1:4000; Molecular Probes, Eugene, OR) for 1 hr at 37°C. The epithelia were rinsed twice with PBS for 10 min each and mounted onto glass slides using Vectashield (Vector Laboratories Inc., Burlingame, CA). Staining was evaluated by laser scanning confocal microscopy (MRC-1024; BioRad) at 60× magnification; images are shown are single 0.5 μm sections.

Immunoprecipitation experiments were done with A549 cells incubated for 30 min at 4°C with lysis buffer (1% Triton X-100, 10 mM Tris-HCl, [pH 7.4], 150 mM NaCl), supplemented with protease inhibitors (10 μg/ml each of leupeptin, aprotinin, and pepstatin A). Samples were precleared by incubating with Protein-A sepharose (1:50; Pierce) for 45 min at 4°C, spun for 5 min at 14,000 rpm, and treated with anti-CAR (1:10) or anti-β-catenin antibody (1:50) for 3 hr at 4°C. Then samples were incubated with rabbit α-mouse IgG (1:100) and Protein-A sepharose (1:20) for 1 hr at 4°C. Precipitants were washed three times with lysis buffer, resuspended in sample buffer, and heated for 5 min at 4°C. Samples were run on SDS-Page gels, transferred to nitrocellulose, and blotted with either anti-β-catenin (1:100) or anti-CAR (1:10) by standard methods. Control samples did not receive primary antibody in the precipitation experiment. Adenovirus preps and epithelial lysate boiled for 5 min at 100°C were run under denaturing conditions on SDS-Page gels. Gels were transferred to nitrocellulose and blotted with either serum (1:100) or serum purified over a fiber-knob affinity column using standard methods.

Dot blots of wild-type adenovirus were performed on fluid collected by rinsing epithelia with EMEM for 30 min at 37°C. Samples were subjected to 3 freeze/thaw cycles and blotted onto a nylon membrane (Ambion, Austin, TX). Adenovirus DNA was detected by hybridizing with a ^{32}P-labeled cDNA probe. Unhybridized probe was washed twice with 2 × SSC and 0.1% SDS at room temperature for 15 min, and once with 0.5 × SSC and 0.1% SDS at 55°C for 1 hr. Dot blots were developed and quantitated using a PhosphorImager (Molecular Dynamics).

Data Analysis

Statistical significance was determined using the student's t test. P values less than 0.05 were considered statistically significant. Data are shown as mean ± standard error of the mean.

Acknowledgments

We thank Phil Karp, Pary Weber, Janice Launspach, Tamara Nesselhauf, Michael Seiler, and Theresa Mayhew for excellent assistance. We thank Karen Springer for preparation of sCAR and fiber-knob proteins. We thank Dr. Klaus Ebner for the generous gift of JAM antibody. We thank Drs. Wouter van't Hof, Soren Leonard, Lance Prince, and John Lee for discussions. We appreciate the help of the Iowa Donor Network. We thank the University of Iowa In Vitro Models and Cell Culture Core and The University of Iowa Vector Core (both supported in part by the National Heart, Lung, and Blood Institute, the Cystic Fibrosis Foundation, and the National Institutes of Diabetes and Digestive and Kidney Diseases), the University of Iowa Central Microscopy Research Facility, the Diabetes and Endocrine Research Center DNA Core (NIH # DK25295), and the Hybridoma/Tissue Culture Facility. This work was supported by the National Heart Lung and Blood Institute, the Cystic Fibrosis Foundation, and the Howard Hughes Medical Institute. P.F. is supported by NIH grant # AI36251. M.J.W. is an Investigator of the Howard Hughes Medical Institute.

Received: April 15, 2002
Revised: August 2, 2002

References

Baranowski, E., Ruiz-Jarabo, C.M., and Domingo, E. (2001). Evolution of cell recognition by viruses. Science *292*, 1102–1105.

Barton, E.S., Forrest, J.C., Connolly, J.L., Chappell, J.D., Liu, Y., Schnell, F.J., Nusrat, A., Parkos, C.A., and Dermody, T.S. (2001). Junction adhesion molecule is a receptor for reovirus. Cell *104*, 441–451.

Bergelson, J.M., Cunningham, J.A., Droguett, G., Kurt-Jones, E.A., Krithivas, A., Hong, J.S., Horwitz, M.S., Crowell, R.L., and Finberg, R.W. (1997). Isolation of a common receptor for coxsackie B viruses and adenoviruses 2 and *5*. Science *275*, 1320–1323.

Bewley, M.C., Springer, K., Zhang, Y.B., Freimuth, P., and Flanagan, J.M. (1999). Structural analysis of the mechanism of adenovirus binding to its human cellular receptor, CAR. Science *286*, 1579–1583.

Boulanger, P.A., and Puvion, F. (1973). Large-scale preparation of soluble adenovirus hexon, penton and fiber antigens in highly purified form. Eur. J. Biochem. *39*, 37–42.

Carson, S.D., Hobbs, J.T., Tracy, S.M., and Chapman, N.M. (1999). Expression of the coxsackievirus and adenovirus receptor in cultured human umbilical vein endothelial cells: regulation in response to cell density. J. Virol. *73*, 7077–7079.

Cohen, C.J., Shieh, J.T., Pickles, R.J., Okegawa, T., Hsieh, J.T., and Bergelson, J.M. (2001). The coxsackievirus and adenovirus receptor is a transmembrane component of the tight junction. Proc. Natl. Acad. Sci. USA *98*, 15191–15196.

Compans, R.W. (1995). Virus entry and release in polarized epithelial cells. Curr. Top. Microbiol. Immunol. *202*, 209–219.

Duan, D., Yue, Y., Yan, Z., McCray, P.B., and Engelhardt, J.F. (1998). Polarity influences the efficiency of recombinant adenoassociated virus infection in differentiated airway epithelia. Hum. Gene Ther. *9*, 2761–2776.

Freimuth, P., Springer, K., Berard, C., Hainfeld, J., Bewley, M., and Flanagan, J. (1999). Coxsackievirus and adenovirus receptor amino-terminal immunoglobulin V-related domain binds adenovirus type 2 and fiber knob from adenovirus type *12*. J. Virol. *73*, 1392–1398.

Geraghty, R.J., Krummenacher, C., Cohen, G.H., Eisenberg, R.J., and Spear, P.G. (1998). Entry of alphaherpesviruses mediated by poliovirus receptor-related protein 1 and poliovirus receptor. Science *280*, 1618–1620.

Greve, J.M., Davis, G., Meyer, A.M., Forte, C.P., Yost, S.C., Marlor, C.W., Kamarck, M.E., and McClelland, A. (1989). The major human rhinovirus receptor is ICAM-1. Cell *56*, 839–847.

Gumbiner, B.M. (1996). Cell adhesion: the molecular basis of tissue architecture and morphogenesis. Cell *84*, 345–357.

Henry, L.J., Xia, D., Wilke, M.E., Deisenhofer, J., and Gerard, R.D. (1994). Characterization of the knob domain of the adenovirus type 5 fiber protein expressed in *Escherichia coli*. J. Virol. *68*, 5239–5246.

Hirst, G.K. (1950). Receptor destruction by viruses of the mumps-NDV-influenza group. J. Exp. Med. *91*, 161–176.

Honda, T., Saitoh, H., Masuko, M., Katagiri-Abe, T., Tominaga, K., Kozakai, I., Kobayashi, K., Kumanishi, T., Watanabe, Y.G., Odani, S., and Kuwano, R. (2000). The coxsackievirus-adenovirus receptor protein as a cell adhesion molecule in the developing mouse brain. Brain Res. Mol. Brain Res. *77*, 19–28.

Horwitz, M.S. (1990). Adenovirus. In Virology, B.N. Fields, D.M. Knipe, D.E. Griffin, R.A. Lamb, M.A. Martin, B. Roizman, and S.E. Straus, eds. (New York: Raven Press), pp. 1723–1740.

Huber, A.H., and Weis, W.I. (2001). The structure of the β-catenin/E-cadherin complex and the molecular basis of diverse ligand recognition by β-catenin. Cell *105*, 391–402.

Huebner, R.J., Rowe, W.P., Ward, T.G., Parrott, R.H., and Bell, J.A. (1954). Adenoidal-pharyngeal-conjunctival agents: a newly recognized group of common viruses of the respiratory system. N. Engl. J. Med. *251*, 1077–1086.

Itoh, M., Sasaki, H., Furuse, M., Ozaki, H., Kita, T., and Tsukita, S. (2001). Junctional adhesion molecule (JAM) binds to PAR-3: a possible mechanism for the recruitment of PAR-3 to tight junctions. J. Cell Biol. *154*, 491–497.

Karp, P.H., Moninger, T.O., Weber, S.P., Nesselhaug, T.S., Launspach, J., Zabner, J., and Welsh, M. (2002). Developing an *in vitro* model of differentiated human airway epithelia: methods for establishing primary cultures. In Epithelial Cell Culture Protocols, C. Wise, ed. (Totowa, NJ: Humana Press, Inc.), pp. 115–137.

Liang, T.W., DeMarco, R.A., Mrsny, R.J., Gurney, A., Gray, A., Hooley, J., Aaron, H.L., Huang, A., Klassen, T., Tumas, D.B., and Fong, S. (2000). Characterization of huJAM: evidence for involvement in cell-cell contact and tight junction regulation. Am. J. Physiol. Cell Physiol. *279*, C1733–C1743.

Louis, N., Fender, P., Barge, A., Kitts, P., and Chroboczek, J. (1994). Cell-binding domain of adenovirus serotype 2 fiber. J. Virol. *68*, 4104–4106.

Pickles, R.J., McCarty, D., Matsui, H., Hart, P.J., Randell, S.H., and Boucher, R.C. (1998). Limited entry of adenovirus vectors into well-differentiated airway epithelium is responsible for inefficient gene transfer. J. Virol. *72*, 6014–6023.

Rajasekaran, A.K., Hojo, M., Huima, T., and Rodriguez-Boulan, E. (1996). Catenins and zonula occludens-1 form a complex during early stages in the assembly of tight junctions. J. Cell Biol. *132*, 451–463.

Rodriquez-Boulan, E., and Sabatini, D.D. (1978). Asymmetric budding of viruses in epithelial monlayers: a model system for study of epithelial polarity. Proc. Natl. Acad. Sci. USA *75*, 5071–5075.

Santis, G., Legrand, V., Hong, S.S., Davison, E., Kirby, I., Imler, J.L., Finberg, R.W., Bergelson, J.M., Mehtali, M., and Boulanger, P. (1999). Molecular determinants of adenovirus serotype 5 fibre binding to its cellular receptor CAR. J. Gen. Virol. *80*, 1519–1527.

Schneider-Schaulies, J. (2000). Cellular receptors for viruses: links to tropism and pathogenesis. J. Gen. Virol. *81*, 1413–1429.

Staunton, D.E., Merluzzi, V.J., Rothlein, R., Barton, R., Marlin, S.D., and Springer, T.A. (1989). A cell adhesion molecule, ICAM-1, is the major surface receptor for rhinoviruses. Cell *56*, 849–853.

Teodoro, J.G., and Branton, P.E. (1997). Regulation of apoptosis by viral gene products. J. Virol. *71*, 1739–1746.

Tsukita, S., Furuse, M., and Itoh, M. (2001). Multifunctional strands in tight junctions. Nat. Rev. Mol. Cell. Biol. *2*, 285–293.

van Raaij, M.J., Chouin, E., van der Zandt, H., Bergelson, J.M., and Cusack, S. (2000). Dimeric structure of the coxsackievirus and adenovirus receptor D1 domain at 1.7 A resolution. Struct. Fold. Des. *8*, 1147–1155.

van't Hof and Crystal, R.G. (2001). Manipulation of the cytoplasmic and transmembrane domains alters the cell surface levels of the coxsackie-adenovirus receptor and changes the efficiency of adenovirus infection. Hum. Gene Ther. *12*, 25–34.

Walters, R.W., Grunst, T., Bergelson, J.M., Finberg, R.W., Welsh, M.J., and Zabner, J. (1999). Basolateral localization of fiber receptors limits adenovirus infection from the apical surface of airway epithelia. J. Biol. Chem. *274*, 10219–10226.

Wang, G., Davidson, B.L., Melchert, P., Slepushkin, V.A., van Es, H.H., Bodner, M., Jolly, D.J., and McCray, P.B.J. (1998). Influence of cell polarity on retrovirus-mediated gene transfer to differentiated human airway epithelia. J. Virol. *72*, 9818–9826.

Welsh, M.J. (1999). Gene transfer for cystic fibrosis. J. Clin. Invest. *104*, 1165–1166.

White, J.M., and Littman, D.R. (1989). Viral receptors of the immunoglobulin superfamily. Cell *56*, 725–728.

Zabner, J., Zeiher, B.G., Friedman, E., and Welsh, M.J. (1996). Adenovirus-mediated gene transfer to ciliated airway epithelia requires prolonged incubation time. J. Virol. *70*, 6994–7003.

Zabner, J., Freimuth, P., Puga, A., Fabrega, A., and Welsh, M.J. (1997). Lack of high affinity fiber receptor activity explains the resistance of ciliated airway epithelia to adenovirus infection. J. Clin. Invest. *100*, 1144–1149.